Available online at www.sciencedirect.com
ScienceDirect
Chinese Journal of Natural Medicines 2021, **19**(11): 874-880
doi: 10.1016/S1875-5364(21)60095-X
Chinese Journal of Natural Medicines

•Research article•

Cytotoxic diaporindene and tenellone derivatives from the fungus *Phomopsis lithocarpus*

LIU Hui-Bo[1, 2Δ], LIU Zhao-Ming[1Δ], CHEN Yu-Chan[1], Tan Hai-Bo[3], LI Sai-Ni[1], LI Dong-Li[2], LIU Hong-Xin[1*], ZHANG Wei-Min[1*]

[1] *State Key Laboratory of Applied Microbiology Southern China, Guangdong Provincial Key Laboratory of Microbial Culture Collection and Application, Guangdong Open Laboratory of Applied Microbiology, Institute of Microbiology, Guangdong Academy of Sciences, Guangzhou 510070, China;*

[2] *School of Chemical and Environmental Engineering, Wuyi University, Jiangmen 529020, China;*

[3] *Program for Natural Products Chemical Biology, Key Laboratory of Plant Resources Conservation and Sustainable Utilization, Guangdong Provincial Key Laboratory of Applied Botany, South China Botanical Garden, Chinese Academy of Sciences, Guangzhou 510650, China*

Available online 20 Nov., 2021

[ABSTRACT] Nine new compounds, including five natural rarely-occurring 2, 3-dihydro-1*H*-indene derivatives named diaporindenes E−I (**1**−**5**), and four new benzophenone analogues named tenellones J−M (**6**−**9**) were isolated from the deep-sea sediment-derived fungus *Phomopsis lithocarpus* FS508. All the structures for these new compounds were fully characterized on the basis of spectroscopic data, NMR spectra, and ECD calculation and single-crystal X-ray diffraction analysis. The potential anti-tumor activities of compounds **1**−**9** against four tumor cell lines SF-268, MCF-7, HepG-2, and A549 were evaluated using the SRB method. Compound **7** exhibited cytotoxic activity against the SF-268 cell line with an IC_{50} value of 11.36 μmol·L^{-1}.

[KEY WORDS] Deep-see-derived fungus; *Phomopsis lithocarpus*; 2, 3-Dihydro-1*H*-indene isomers; Benzophenone derivatives
[CLC Number] R284 **[Document code]** A **[Article ID]** 2095-6975(2021)11-0874-07

Introduction

Nowadays, marine natural products have emerged as one of the most important strategic sources for drug discovery and pharmaceutical usage. Their diverse structures and pharmacological effects in medical industry have been significantly reflected by the fruitful achievements for bioactive natural products [1-2]. Moreover, the therapeutic potential of marine natural products have also been further immensely advanced with the tremendous efforts in synthetic and pharmaceutical communities towards their total synthesis and structure-activity relationship studies [3-5]. Many bioactive natural products produced by marine fungi and their semi-synthetic analogues have been entered in clinical research or commercially available on the market, such as plinabulin, cephalosporins, myriocin, and fingolimod [6-8].

The fungal genus *Phomopsis* has been proven as a rich source of natural products with diverse structures, many of which display a broad spectrum of attractive biological activities including anti-viral [9], immunosuppressive [10], anti-fungal [11], anti-inflammatory [12,13], anti-oxidation [14], anti-tumor [15], anti-microbial [16], motility inhibitory and zoosporicidal activities [17], and enzyme inhibition activities [18]. Inspired by the significant achievements on natural product chemistry from marine fungi, our research group focuses on screening and developing structurally diverse bioactive secondary metabolites [19-23]. As part of our ongoing investigation of *P. lithocarpus* FS508, extensive research was conducted, obtaining five unusual 2, 3-dihydro-1*H*-indene isomers named diaporindenes E−I (**1**−**5**), and four new benzophenone derivatives designated as tenellones J−M (**6**−**9**) (Fig. 1).

[Received on] 18-Mar.-2021
[Research funding] This work was supported by Guangdong Provincial Special Fund for Marine Economic Development Project (No. GDNRC[2020]042), the National Natural Science Foundation of China (No. 41906106), Guangdong Special Support Program (No. 2019TQ05Y375), the Team Project of the Natural Science Foundation of Guangdong Province (No. 2016A030312014), and the GDAS' Project of Science and Technology Development (No. 2019GDASYL-0103007).
[*]**Corresponding author]** E-mails: liuhx@gdim.cn (LIU Hong-Xin); wmzhang@gdim.cn (ZHANG Wei-Min)
[Δ]These authors contributed equally to this work.
These authors have no conflict of interest to declare.

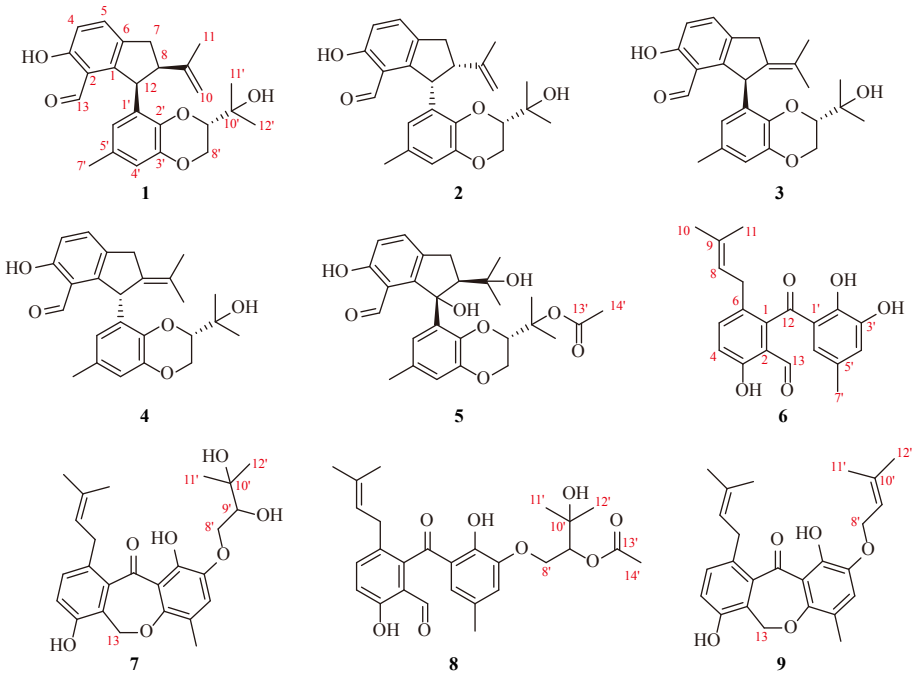

Fig. 1 Structures of compounds 1−9

Herein, the details of isolation, structural elucidation by NMR spectral interpretation, quantum molecular calculation, X-ray diffraction, and biological evaluation were described.

Results and Discussion

Diaporindene E (**1**) was obtained as white needles. Its molecular formula was determined as $C_{25}H_{28}O_5$ on the basis of positive HR-ESI-MS data with a molecular ion at *m*/*z* 409.2011 $[M + H]^+$ (Calcd. for $C_{25}H_{29}O_5$, 409.2010), indicating the existence of 12 indices of hydrogen deficiency. The IR spectrum of **1** showed two unambiguous absorption bands at 3354 and 1651 cm^{-1}, which were the characteristics of hydroxy and carbonyl functionalities, respectively. With careful interpretation of its ^{13}C NMR (Table S6) and HSQC spectra, 25 carbon signals were successfully distinguished and ascribed to a carbonyl moiety, four methyls, three methylenes, seven methines, and ten quaternary carbons.

The proton-proton connectivity of **1** clearly clarified the existence of three spin-coupling systems: **a** (H-4/H-5), **b** (H-7/H-8/H-12), and **c** (H-8′/H-9′) as depicted in Fig. 2. These spectroscopic features were similar to those of the known compound diaporindene A [24], excepting for the presence of two olefinic carbons (δ_C 111.8, 145.0) as well as the absence of a methyl functional group and a quaternary carbon in **1**, which strongly suggested that the 1-propoxy unit should be replaced by an isopropenyl unit. The aforementioned deduction was further established by the HMBC correlations from H_2-10 and H_3-11 to C-8 and C-9, H-4 to C-2 and C-6, as well as H-5 to C-3, C-1, and C-7 along with the spin-coupling system **b** from the COSY spectrum. Moreover, the HMBC and COSY correlations as shown in Fig. 2 indicated that the propan-2-ol fragment was linked to 2, 3-dihydrobenzo[*b*][1, 4]dioxine moiety.

Likewise, the 2, 3-dihydrobenzo[*b*][1,4]dioxine moiety could be unambiguously confirmed by the key HMBC correlations from the cross-peaks of H-4′/C-2′, C-3′, and C-7′ in conjunction with H-7′ to C-2′ as referring to the substructure **c**. Additionally, the aldehyde functionality could be readily located at C-2 position by the critical HMBC correlations from H-13 to C-2 and C-3. Furthermore, the HMBC correlations from H_3-7′ to C-4′, C-5′, and C-6′ chemo-logically evidenced that the C-7′ methyl functional group was connected to the aromatic phenyl ring at C-5′. Based on the above informative deduction, the planar structure was finally elucidated as shown in Fig. 1. The obvious NOESY correlation of H-12/H-7*α* and H-7*β*/H_3-11 suggested that H-12 and H-8 were co-facial and arbitrarily assigned to be *α*-orientation. In order to substantiate the above deduction and establish the stereochemistry of **1**, the X-ray single-crystallographic analysis was conducted. Fortunately, the single crystals were obtained from a MeOH-H_2O solvent system, and an X-ray diffraction experiment was performed with CuK*α* radiation (Fig. 3). The crystal data unambiguously assigned its absolute configuration as 8*R*,12*R*,9′*S*. Finally, the structure of **1** was determined and given the trivial name as diaporindene E.

Diaporindene F (**2**) was obtained as yellow oil with the molecular formula of $C_{25}H_{28}O_5$ deduced from the HR-ESI-MS. The ^{13}C NMR (Table S6) and HSQC spectra of **2** showed 25 carbon signals, which displayed very close similarity in most profiles of chemical shifts for those of **1**. The slight differences of the NMR chemical shifts (upshifted or downshifted) between **2** and **1** were clearly distinguished in Table S6. These data logically indicated that compounds **2** and **1** shared the same carbon core skeleton, and the vari-

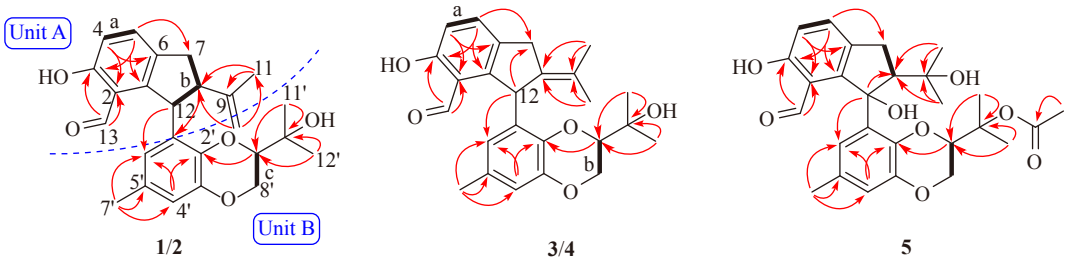

Fig. 2 ^{1}H-^{1}H COSYs and key HMBCs of 1−5

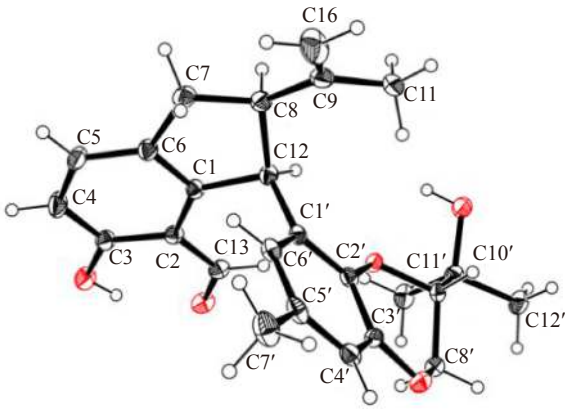

Fig. 3 X-ray crystallographic analysis of 1

ations of chemical shifts for those carbons might be due to the presence of different chiral genetic centers. Therefore, the planar structure of **2** was tentatively assigned to be the same as **1** shown in Fig. 1.

In the NOESY spectrum, the key NOE correlations of H-12/H-7α strongly suggested that these protons should be co-facial and arbitrarily assigned to be in α-orientation. Meanwhile, the NOE correlation of H-7β/H$_3$-11 indicated that the isopentyl group was β-orientation. Compound **2** displayed a reversal and symmetric ECD absorption curve comparing to **1** (Fig. S1), which strongly suggested that the absolute configurations of the C-8 and C-12 stereogenic centers, close to critical chromophores in **2**, was opposite to those of compound **1**, thus tentatively deducing to be 8*S* and 12*S*. With respect to the same biosynthetic pathway and the weak ECD absorption of C-9′ stereogenic center at 200−300 nm for this kind of compounds, the absolute configuration of C-9′ stereogenic center for **2** was assumed to be identical to that of compound **1**. Moreover, the absolute configuration of **2** was further confirmed by the ECD calculations. As showed in Fig. S1, the calculated ECD curve of 8*S*, 12*S*, 9′*S*-**2** was perfectly consistent with the experimental curve, which successfully evidenced the aforementioned deduction. Thus, the absolute configuration of **2** was determined as 8*S*, 12*S*, 9′*S* and given the trivial name diaporindene F.

Diaporindene G (**3**) was obtained as yellow needles. The molecular formula was assigned as $C_{25}H_{28}O_5$ based on the positive mode with the HR-ESI-MS $[M + H]^+$ ion discovered at *m*/*z* 409.2008 (Calcd. for 409.2010), indicating the presence of 12 degrees of unsaturation in the molecule. The ^{1}H and ^{13}C NMR spectra of **3** closely resembled to those of **1** except for the presence of an additional methyl functionality ($\delta_{H/C}$ 1.56/20.2) and the absence of a methine carbon in **3**, which collectively indicated that the double bond of C-9/C-10 might be rearranged to be the olefin at the carbons C-8/C-9; these findings were confirmed by the HMBC correlations from H$_3$-10 (δ_C 20.2) and H$_3$-11 (δ_C 21.8) to C-8 (δ_C 135.8) and C-9 (δ_C 126.8). Thus, the planar structure of **3** was unambiguously elucidated as depicted in Fig. 1.

Diaporindene H (**4**) was obtained as white needles with the molecular formula of $C_{25}H_{28}O_5$ as deduced from the HR-ESI-MS spectrum. Similar to compound **3**, the ^{13}C NMR data as shown in Table S7 and HSQC spectrum of **4** also showed 25 carbon signals. Moreover, the chemical shifts for all the carbons displayed close similarity with those of compound **3**. The slight differences of the NMR chemical shifts between **4** and **3** were clearly distinguished in the NMR data (Table S7), which strongly suggested that these two compounds existed as a pair of related diastereoisomers. The absolute structures of compounds **3** and **4** were established as 12*S*, 9′*S* and 12*R*,9′*S* respectively by ECD calculations as shown in Figs. S2 and S3. Therefore, the final structure of **4** was determined to be the diastereoisomer of compound **3** and given the trivial name as diaporindene H.

Diaporindene I (**5**) was purified as white powder. Its molecular formula was assigned as $C_{27}H_{32}O_8$ based on the positive mode with a HR-ESI-MS $[M + H]^+$ ion peak at *m*/*z* 485.2160 (Calcd. for 485.2170). The 1D NMR data (Table S8) of **5** was similar to those of **1**, indicating that **5** should also share a very similar diaporindene skeleton. After careful inspection of their 1D NMR data, the major differences between **1** and **5** were disclosed to be the presence of an acetyl moiety (δ_C 22.0, 170.3) and the absence of two olefinic carbons in **5**. The HMBC correlations of H$_3$-10 (δ_H 1.51) and H$_3$-11 (δ_H 1.52) to C-8 (δ_C 53.7) and C-9 (δ_C 84.8) strongly suggested that the 2-propenyl functional group should be replaced by a propan-2-ol unit, which was further confirmed by the up-shifted carbon resonances for C-9 (δ_C 84.8) and C-10 (δ_C 27.1). Similarly, the down-shifted quaternary carbon resonance for C-12 (δ_C 84.2) confirmed that the hydroxyl moiety should link at C-12 position. As referring to the NOESY cross peaks of H-14′/H-11′ and H-14′/H-12′, the HMBC correlation from H-14′ to C-13′ strongly suggested the acetoxy functionality to be located at C-10′ position.

The relative configuration of compound **5** was investig-

ated by the NOESY experiment. In the NOESY spectrum, the cross peak of H-8 (δ_H 3.87)/H-7α (δ_H 2.90) suggested that they were cofacial and arbitrarily assigned as α-orientation. Thus, the partial relative configuration of compound **5** was determined as depicted in Fig. 2 and given a trivial name as diaporindene I. Finally, the absolute configuration of compound **5** was determined as 8*R*,12*R*,9′*S* by ECD calculation as shown in Fig. S4.

Tenellone J (**6**) was obtained as purple powder, and its molecular formula was assigned as $C_{20}H_{20}O_5$ based on the negative mode HR-ESI-MS with an obvious molecular ion peak at *m*/*z* 339.1225 $[M - H]^-$ (Calcd. for $C_{20}H_{19}O_5$, 339.1238), which corresponded to 11 indices of hydrogen deficiency. With careful inspection and analysis of its ^{13}C NMR (Table S9) and HSQC spectra, 20 carbon signals were successfully distinguished and ascribed to two carbonyl moieties, three methyls, a methylene, five methines, and nine quaternary carbons.

The proton-proton connectives of **6** clearly clarified the existence of two spin-coupling systems: **a** (H-4/H-5) and **b** (H-7/H-8) as depicted in Fig. 2. On the basis of fragment **a**, a 1,2,3,6-tetrasubstituted aromatic ring was initially established by the critical HMBC correlations from H-4 to C-2 and C-6 as well as H-5 to C-1 and C-3. Moreover, the HMBC correlations from H-10 and H-11 to C-9 and C-8, coupled with the fragment **b**, strongly suggested the presence of an isopentenyl fragment; and it was concluded to link at C-6 (δ_C 129.6) position in the 1, 2, 3, 6-tetrasubstituted aromatic ring. The aforementioned conclusion could be further evidenced by the pivotal HMBC interaction from the methylene protons H-7 (δ_H 3.13) to C-5. Similarly, the location of the C-13 aldehyde group (δ_C 194.3) at C-2 (δ_C 117.3) position in the aromatic ring was reasonably verified by the conclusive HMBC correlations from the aldehyde proton H-13 (δ_H 9.72) to C-1, C-2, and C-3. The position of the hydroxyl group linked at C-3 mainly referred to its significant down-shifted carbon signal at δ_C 160.7. Therefore, the unit A was finally established as shown in Fig. 2.

In unit B, the second 1′, 2′, 3′, 5′-tetrasustituted benzene ring with a phenolic group C-2′ (δ_C 147.6) was readily constructed by the *meta*-coupled aromatic protons of H-4′ (δ_H 7.02) and H-6′ (δ_H 6.45). The aforementioned conclusion was further confirmed and supported by the HMBC interactions of H-4′ to C-2′, H-4′ to C-6′, as well as H-6′ to C-4′. In addition, the HMBC correlations from H-7′ (δ_H 2.16) to C-4′, C-5′, and C-6′ strongly suggested the location of the methyl group at C-5′ (δ_C 129.6) position. Moreover, the quaternary and down-shifted carbon signal at C-3′ (δ_C 145.3) also strengthened the deduction that a hydroxyl group might link at C-3′ position. Therefore, the unit B was completely ascertained.

The connectivity of the units A and B was initially speculated to conjunct through the carbonyl carbon atom C-12 (δ_C 203.2) with the formation of a benzophenone architecture, which mainly referred to the HMBC correlation between H-6′ and C-12 as well as correlation from H-5 to C-12. In light of the aforementioned findings, the structure of **6** was concluded as shown in Fig. 2 and given the trivial name as tenellone J.

Tenellone K (**7**) was isolated as yellow oil. Its molecular formula was assigned as $C_{25}H_{30}O_7$ based on the positive HR-ESI-MS mode with a molecular ion shown at *m*/*z* 465.1877 $[M + Na]^+$ (Calcd. for $C_{25}H_{30}NaO_7$, 465.1884), indicating the presence of 11 degrees of unsaturation in the molecule. Compared the NMR data between compounds **6** and **7**, it was concluded that compound **7** was also a tenellone derivative. The NMR data of compound **7** were similar with those of the known compound tenellone A [23], where the main differences between them were that the aldehyde group in tenellone A was replaced by a hydroxymethyl one and the C-6′ methine carbon was replaced by an oxygenated quaternary carbon. These deduction was further evidenced and supported by the carbon shift of C-13 (δ_C 65.4) and the HMBC correlations from H_2-13 to C-1, C-3 and C-6′. Thus, the structure of **7** was concluded as shown inFig. 2 and given the trivial name as tenellone K.

Tenellone L (**8**) was also obtained as yellow oil. Its molecular formula was deduced as $C_{27}H_{32}O_8$ on the basis of the positive HR-ESI-MS data with a molecular ion at *m*/*z* 485.2173 $[M + H]^+$ (Calcd. for $C_{17}H_{25}O_4$, 485.2170). A detailed inspection and comparison of the 1D NMR spectra between **8** and **6** clearly revealed that both of them possessed the same benzophenone architecture, which was further confirmed by the 2D NMR correlations. The notable differences between the two compounds were ascribed to the presence of seven additional carbons (δ_C 20.8, 25.7, 26.0, 69.7, 71.3, 77.9, 170.6) in **8**, which were the characteristics for an isopentyl moiety and an acetoxy functionality. The HMBC correlations of H_3-14′ to C-13′, H-9′ to C-13′ suggested that the acetoxy functionality might be located at C-9′ position, whereas the informative HMBC correlation from H_2-8′ to C-3′ verified the attachment of the highly oxygenated isopentyl moiety at C-3′ in the benzophenone architecture. Thus, compound **8** was finally determined and given the trivial name as tenellone L.

Tenellone M (**9**) was obtained as yellow needles. Its molecular formula was assigned as $C_{25}H_{28}O_5$ based on the positive HR-ESI-MS mode with a molecular ion at *m*/*z* 409.2012 $[M + H]^+$ (Calcd. for $C_{25}H_{29}O_5$, 409.2010). The 1D NMR data (Table S10) of **9** were similar to those of the known compound tenellone D [23], indicating that they should also share a very similar tenellone skeleton, except for the absence of the aldehyde moiety in conjunction with the presence of an oxygenated methylene (δ_C 65.2) in **9**. This deduction could be further rationalized by the critical HMBC correlations from H_2-13 (δ_H 5.22) to C-1 (δ_C 140.7), C-2 (δ_C 122.8), C-1′ (δ_C 150.8), and C-6′ (δ_C 153.1), which strongly suggested that the aldehyde moiety was replaced by the oxygenated methylene group, which ought to be linked at C-6′ position in the benzene ring. Therefore, compound **9** was fi-

nally determined and given the trivial name as tenellone M.

Compounds **1**−**9** were evaluated for their cytotoxic activities against the SF-268, MCF-7, HepG-2, and A-549 tumor cell lines, with cisplatin as the positive control. Compound **7** exhibited moderate inhibitory activity against SF-268 cell line with an IC_{50} value of 11.36 μmol·L^{-1}, as well as weak inhibitory activity against HepG-2 and A-549 cell lines with IC_{50} values of 34.85 and 47.60 μmol·L^{-1}, respectively. Meanwhile, compounds **4**, **6**, and **9** showed weak inhibitory effects against SF-268 cell line with the IC_{50} values ranging from 29.49 to 44.48 μmol·L^{-1}. The other five compounds exhibited no cytotoxic activity even at the concentration of 50 μmol·L^{-1} (Table 1).

Conclusion

In summary, five 2, 3-dihydro-1*H*-indene isomers and four new benzophenone derivatives, were isolated from the marine-derived fungus *P. lithocarpus* FS508. The chemical structures of nine compounds were elucidated by NMR analysis. The anti-tumor activities of compounds **1**−**9** were evaluated, wherein compound **7** exhibited moderate growth inhibitory effects against SF-268 cell line with an IC_{50} value of 11.36 μmol·L^{-1}, as well as weak inhibitory activity against HepG-2 and A-549 cell lines with IC_{50} values of 34.85 and 47.60 μmol·L^{-1}, respectively. Meanwhile, compounds **4**, **6**, and **9** displayed weak inhibitory effects against SF-268 cell line with the IC_{50} values ranging from 29.49 to 44.48 μmol·L^{-1}. However, the other five compounds did not exhibit cytotoxic activity against these tumor cell lines even at 50 μmol·L^{-1}.

Experimental

General procedures

UV spectra were taken on a Shimadzu UV-2600 spectrophotometer (Shimadzu, kyoto, Japan). IR data were recorded on a Shimadzu IR Affinity-1 spectrometer (Shimadzu, Kyoto, Japan). Optical rotation values were measured on an Anton Paar MCP-500 spectroplarimeter (Anton Paar, Graz, Austria) at 25 °C. Circular dichroism (CD) spectra were obtained under N_2 gas on a Jasco 820 spectropolarimeter (Jasco Corporation, Kyoto, Japan). The NMR spectra were acquired using a Bruker Avance 600 MHz NMR spectrometer with TMS as an internal standard (Bruker, Fallanden, Switzerland). ESI-MS data were collected on an Agilent Technologies 1290-6430A Triple Quad LC/MS (Agilent Technologies, Palo Alto, CA, USA). HR-ESI-MS were done with a Thermo MAT95XP high resolution mass spectrometer (Thermo Fisher Scientific, Bremen, Germany). Preparative HPLC separation were carried out using a YMC-pack ODS-A column (250 mm × 20 mm, 5 μm, 12 nm, YMC Co., Ltd., Kyoto, Japan). Semi-preparative HPLC separation was performed utilizing a YMC-pack ODS-A/AQ column (250 mm × 10 mm, 5 μm, 12 nm, YMC Co., Ltd., Kyoto, Japan), a S-Chiral A column (250 mm × 10 mm, 5 μm, 12 nm, Acchrom Technologies Co., Ltd., Beijing, China) and a YMC-pack Cellulose-SB column (250 mm × 10 mm, 5 μm, 12 nm, YMC Co., Ltd., Kyoto, Japan). Column chromatography was performed with silica gel (200−300 mesh, Qingdao Marine Chemical Inc., Qingdao, China) and Sephadex LH-20 (Amersham Biosciences, Uppsala, Sweden), respectively. Thin-layer chromatography (TLC) was conducted with precoated glass plates GF-254 (Merck KGaA, Darmastadt, Germany).

Fungal material

The fungus *P. lithocarous* FS508 was isolated in 2016 from a deep-sea sediment sample collected in Indian Ocean (111°53.335′ E, 16°50.508′ N; depth 3606 m). The sequence of amplified ITS region of the strain FS508 has been submitted to GenBank (Accession No. MG686131). A BLAST search of ITS region revealed that FS508 has 99% homology with *Phomopsis lithocarpus* CZ105B (Accession No. FJ755236). The strain is preserved at Guangdong Provincial Key Laboratory of Microbial Culture Collection and Application, Guangdong Institute of Microbiology.

Fermentation, extraction, and isolation

The fermentation was carried out in 3 L Erlenmeyer flasks, which contained 250 g of rice and 300 mL of 0.5% saline water. Each flask was aseptically inoculated with the seed inocula and statically fermented at 28°C for a month. The fermented rice substrate (40 flasks) was extracted three times with EtOAc, and the solvent was evaporated to dryness under the vacuum to obtain a crude extract. The crude extract was subjected to silica gel chromatography (200−300 mesh) by step gradient elution with petroleum ether/EtOAc (10 : 1→0 : 1) followed by CH_2Cl_2/MeOH in linear gradient (5 : 1→1 : 1) to yield 8 fractions (Frs. 1−8).

Fr. 3 was further rechromatographed by column chromatography over C_{18} reversed phase (RP) silica gel eluting with a MeOH/H_2O gradient (60 : 40→100 : 0) to produce 4 fractions Fr. 3-1−Fr. 3-4. Fr. 3-3 was further purified by column chromatography on silica gel eluting with a n-hexane/EtOAc

Table 1 Cytotoxic activities of compounds 1-9

Compound	IC_{50} (μmol·L^{-1})[a]			
	SF-268	MCF-7	HepG-2	A549
1	≥ 50	≥ 50	≥ 50	≥ 50
2	≥ 50	≥ 50	≥ 50	≥ 50
3	≥ 50	≥ 50	≥ 50	≥ 50
4	40.25 ± 0.34	≥ 50	≥ 50	≥ 50
5	≥ 50	≥ 50	≥ 50	≥ 50
6	≥ 50	≥ 50	≥ 50	≥ 50
7	11.36 ± 1.52	≥ 50	34.85 ± 2.47	47.60 ± 5.47
8	44.48 ± 0.98	≥ 50	≥ 50	≥ 50
9	29.49 ± 3.69	≥ 50	≥ 50	≥ 50
Cisplatin	3.25 ± 0.05	3.02 ± 0.11	2.13 ± 0.17	2.65 ± 0.03

[a]Values are expressed as the mean ± SD

(5 : 1−3 : 1) to produce 2 fractions Fr. 3-3-1−Fr. 3-3-2. Fr. 3-3-1 was re-purified by HPLC on a semipreparative YMC-pack ODS-A/AQ column (MeCN/H_2O, 80 : 20, 2 mL·min^{-1}) to produce 9 fractions Fr. 3-3-1-1−Fr. 3-3-1-9. Fr. 3-3-1-5 was purified by HPLC on a semipreparative YMC-pack Cellulose-SB column (MeCN/H_2O, 65 : 35, 2 mL·min^{-1}) to produce 5 fractions Fr. 3-3-1-5-1−Fr. 3-3-1-5-5, and **3** (2.0 mg, t_R 18.4 min) was obtained from Fr. 3-3-1-5-5. Fr. 3-3-1-5-3 was re-purified by HPLC on a semipreparative S-Chiral A column (*n*-hexane/2-propanol, 9 : 1, 2 mL·min^{-1}) to afford **1** (2.3 mg) and **2** (1.9 mg). Fr. 3-3-1-7 was fractionated by HPLC on a semipreparative YMC-pack Cellulose-SB column (MeCN/H_2O, 70 : 30, 2 mL·min^{-1}) to obtain **9** (1.8 mg, t_R 24.2 min) and **4** (1.3 mg, t_R 23.0 min).

Fr. 5 was separated by column chromatography over C_{18} reversed phase (RP) silica gel eluting with a MeOH/H_2O gradient (80 : 20→100 : 0) to produce 5 fractions Fr. 5-1−Fr.5-5. Fr.5-1 was further fractionated by column chromatography on silica gel eluting with a *n*-hexane/EtOAc (3 : 1→1 : 1) to produce 4 fractions Fr. 5-1-1−Fr. 5-1-4. Fr. 5-1-4 was purified by HPLC on a semipreparative YMC-pack ODS-A/AQ column (MeCN/H_2O, 75 : 25, 2 mL·min^{-1}) to produce 3 fractions Fr. 5-1-4-1−Fr. 5-1-4-3. Fr. 5-1-4-1 was re-purified by HPLC on a semipreparative YMC-pack Cellulose-SB column (MeCN/H_2O, 50 : 50, 2 mL·min^{-1}) to obtain **5** (2.6 mg, t_R 10.7 min). Fr. 5-1-4-3 was re-purified by HPLC on a semipreparative YMC-pack Cellulose-SB column (MeCN/H_2O, 65 : 35, 2 mL·min^{-1}) to obtain **6** (3.5 mg, t_R 15.5 min).

Fr. 6 was separated by column chromatography on silica gel eluting with *n*-hexane/EtOAc (5 : 1→1 : 2) to produce 7 fractions Fr. 6-1−Fr. 6-7. Fr. 6-2 was further fractionated by HPLC on a semipreparative YMC-pack Cellulose-SB column (MeCN/H_2O, 80 : 20, 2 mL·min^{-1}) to obtain **8** (1.8 mg, t_R 16.4 min). Fr. 6-6 was fractionated by column chromatography over C_{18} reversed phase (RP) silica gel eluting with a MeOH/H_2O gradient (70 : 30→100 : 0) to produce 7 fractions Fr.6-6-1−Fr.6-6-7. Fr.6-6-3 was separated by Sephadex LH-20, eluting with CH_2Cl_2/MeOH (1 : 1) to yield 4 fractions Fr. 6-6-3-1−Fr. 6-6-3-4. Fr. 6-6-3-3 was further fractionated by column chromatography on silica gel eluting with *n*-hexane/EtOAc (5 : 1→1 : 1) to produce 7 fractions Fr. 6-6-3-3-1−Fr. 6-6-3-3-7. Fr. 6-6-3-3-4 was purified by HPLC on a preparative YMC-pack ODS-A column (MeOH/H_2O, 80 : 20, 6 mL·min^{-1}) to yield 6 fractions Fr. 6-6-3-3-4-1−Fr. 6-6-3-3-4-6. Fr. 6-6-3-3-4-5 was re-purified by HPLC on a semipreparative YMC-pack ODS-A/AQ column (MeCN/H_2O, 65 : 35, 2 mL·min^{-1}) to afford **7** (1.1 mg, t_R 26.2 min).

Diaporindene E (***1***): white needles; $[\alpha]_D^{25}$ + 61.6 (*c* 0.02, MeOH). UV (MeOH) λ_{max} (log ε) 210 (3.21), 261 (2.44), 353 (2.12) nm; IR ν_{max} 3327, 2947, 2833, 1020, 667 cm^{-1}. ^{1}H (600 MH_Z) and ^{13}C (150 MH_Z) NMR spectral data, see Table S6; positive ESI-MS: *m/z* 409 [M + H]$^+$; HR-ESI-MS *m/z* 409.2011 [M + H]$^+$ (Calcd. for $C_{25}H_{29}O_5$, 409.2010).

Diaporindene F (***2***): yellow oil; $[\alpha]_D^{25}$ − 69.0 (*c* 0.03, MeOH). UV (MeOH) λ_{max} (log ε) 210 (3.33), 262 (2.72), 353 (2.37) nm; IR ν_{max} 3354, 2920, 1651, 1469, 1423, 1020, 690 cm^{-1}. ^{1}H (600 MH_Z) and ^{13}C (150 MH_Z) NMR spectral data, see Table S6; positive ESI-MS: *m/z* 409 [M + H]$^+$; HR-ESI-MS *m/z* 409.2016 [M + H]$^+$ (Calcd. for $C_{25}H_{29}O_5$, 409.2010).

Diaporindene G (***3***): yellow needles; $[\alpha]_D^{25}$ + 39.5 (*c* 0.02, MeOH). UV (MeOH) λ_{max} (log ε) 209 (3.12), 260 (2.32), 350 (1.97) nm; IR ν_{max} 3332, 2947, 2853, 1018, 646 cm^{-1}. ^{1}H (600 MH_Z) and ^{13}C (150 MH_Z) NMR spectral data, see Table S7; positive ESI-MS: *m/z* 409 [M + H]$^+$; HR-ESI-MS *m/z* 409.2008 [M + H]$^+$ (Calcd. for $C_{25}H_{29}O_5$, 409.2010).

Diaporindene H (***4***): white needles; $[\alpha]_D^{25}$ − 24.4 (*c* 0.02, MeOH). UV (MeOH) λ_{max} (log ε) 208 (3.13), 264 (2.31), 349 (1.95) nm; IR ν_{max} 3309, 2949, 2835, 1647, 1016, 667 cm^{-1}. ^{1}H (600 MH_Z) and ^{13}C (150 MH_Z) NMR spectral data, see Table S7; positive ESI-MS: *m/z* 409 [M + H]$^+$; HR-ESI-MS *m/z* 409.2006 [M + H]$^+$ (Calcd. for $C_{25}H_{29}O_5$, 409.2010).

Diaporindene I (***5***): white powder; $[\alpha]_D^{25}$ + 36.5(*c* 0.02, MeOH). UV (MeOH) λ_{max} (log ε) 212 (3.38), 266 (2.85), 351 (2.45) nm; IR ν_{max} 3309, 2947, 2835, 1647, 1541, 1506, 1456, 1018, 665 cm^{-1}. ^{1}H (600 MH_Z) and ^{13}C (150 MH_Z) NMR spectral data, see Table S8; positive ESI-MS: *m/z* 485 [M + H]$^+$; HR-ESI-MS *m/z* 485.2160 [M + H]$^+$ (Calcd. for $C_{27}H_{33}O_8$, 485.2170).

Tenellone J (***6***): purple powder; UV (MeOH) λ_{max} (log ε) 217 (3.51), 267 (3.05), 343 (2.68) nm; IR ν_{max} 3325, 2927, 1653, 1456, 1313, 1271, 1165, 1018, 750 cm^{-1}. ^{1}H (600 MH_Z) and ^{13}C (150 MH_Z) NMR spectral data, see Table S9; negative ESI-MS: *m/z* 339 [M − H]$^-$; HR-ESI-MS *m/z* 339.1225 [M − H]$^-$ (Calcd. for $C_{20}H_{19}O_5$, 339.1238).

Tenellone K (***7***): yellow oil; UV (MeOH) λ_{max} (log ε) 200 (3.59), 221 (3.35), 297 (2.90), 346 (2.55) nm; IR ν_{max} 3354, 1653, 1506, 1456, 1014, 665 cm^{-1}. ^{1}H (600 MH_Z) and ^{13}C (150 MH_Z) NMR spectral data, see Table S9; positive ESI-MS: *m/z* 443 [M + H]$^+$; HR-ESI-MS *m/z* 465.1877 [M + Na]$^+$ (Calcd. for $C_{25}H_{30}NaO_7$, 465.1884).

Tenellone L (***8***):yellow oil; UV (MeOH) λ_{max} (log ε) 222 (3.58), 266 (3.30), 346 (3.05) nm; IR ν_{max} 2974, 2926, 1747, 1651, 1456, 1373, 1265, 1240, 1168, 1037, 775, 752 cm^{-1}. ^{1}H (600 MH_Z) and ^{13}C (150 MH_Z) NMR spectral data, see Table S10; positive ESI-MS: *m/z* 485 [M + H]$^+$; HR-ESI-MS *m/z* 485.2173 [M + H]$^+$ (Calcd. for $C_{27}H_{33}O_8$, 485.2170).

Tenellone M (***9***): yellow needles; UV (MeOH) λ_{max} (log ε) 203 (4.27), 221 (4.04), 298 (3.64), 349 (3.35) nm; IR ν_{max} 3313, 2920, 2833, 1456, 1022, 669 cm^{-1}. ^{1}H (600 MH_Z) and ^{13}C (150 MH_Z) NMR spectral data, see Table S10; positive ESI-MS: *m/z* 409 [M + H]$^+$; HR-ESI-MS *m/z* 409.2012 [M + H]$^+$ (Calcd. for $C_{25}H_{29}O_5$, 409.2010).

X-ray crystallographic analysis of compound 1

A suitable crystal was selected and measured on a XtaLAB AFC12 (RINC): Kappa single diffractometer. The crystal was kept at 100(1) K during data collection. Using Olex2, the structure was solved with the ShelXT structure solution program using Intrinsic Phasing and refined with the ShelXL refinement package using Least Squares minimisa-

tion.

Crystal data for $C_{25}H_{28}O_5$ (M = 408.47 g·mol^{-1}): monoclinic, space group P21 (no. 4), a = 7.746 00(10) Å, b = 21.1808(4) Å, c = 13.0247(2) Å, β = 90.372(2), V = 2136.87(6) Å3, Z = 4, T = 100(1) K, μ(CuKα) = 0.709 mm^{-1}, Dcalc = 1.270 g·cm^{-3}, 21346 reflections measured (7.968 ≤ 2Θ ≤ 134.124°), 7613 unique (Rint = 0.0414, Rsigma = 0.0479) which were used in all calculations. The final R1 was 0.0459 (I > 2σ(I)) and wR2 was 0.1190 (all data). Crystallographic data for **1** reported in this paper has been deposited in the Cambridge Crystallographic Data Centre. (Deposition number: CCDC 2021998). Copies of these data can be obtained free of charge via www.ccdc.cam.au.ck/conts/retrieving.html.)

Cytotoxicity assay

The cytotoxic activities of compounds (**1**−**9**) were evaluated against four human tumor cell lines SF-268, MCF-7, HepG-2, and A549 with cisplatin as the positive control. The cytotoxic tests were performed using the sulforhodamine (SRB) method [25].

References

[1] Jans PE, Mfuh AM, Arman HD, *et al*. Cytotoxicity and mechanism of action of the marine-derived fungal metabolite trichodermamide B and synthetic analogues [J]. *J Nat Prod*, 2017, **80**: 676-683.

[2] Blunt JW, Carroll AR, Copp BR, *et al*. Marine natural products [J]. *Nat Prod Rep*, 2018, **35**: 8-53.

[3] Li XD, Li XM, Xu GM, *et al*. Anti-microbial phenolic bisabolanes and related derivatives from *Penicillium aculeatum* SD-321, a deep sea sediment-derived fungus [J]. *J Nat Prod*, 2015, **78**: 844-849.

[4] Wang C, Guo L, Hao JJ, *et al*. α-Glucosidase inhibitors from the marine-derived fungus *Aspergillus flavipes* HN4-13 [J]. *J Nat Prod*, 2016, **79**: 2977-2981.

[5] Liao LJ, Bae SY, Won TH, *et al*. Aseperphenins A and B, lipopeptidyl benzophenones from a marine-derived *Aspergillys sp*. fungus [J]. *Org Lett*, 2017, **19**: 2066-2069.

[6] Wang YT, Xue YR, Liu CH. A brief review of bioactive metabolites derived from deep-sea fungi [J]. *Mar Drugs*, 2015, **13**: 4594-4616.

[7] Newman DJ, Cragg GM. Natural products as sources of new drugs from 1981 to 2014 [J]. *J Nat Prod*, 2016, **79**: 629-661.

[8] Deshmukh SK, Prakash V, Ranjan N. Marine fungi: a source of potential anti-cancer compounds [J]. *Front Microbiol*, 2018, **8**: 2536.

[9] Xie SS, Wu Y, Qiao YB, *et al*. Protoilludane, illudalane, and botryane sesquiterpenoids from the endophytic fungus *Phomopsis* sp. TJ507A [J]. *J Nat Prod*, 2018, **81**: 1311-1320.

[10] Wei W, Gao J, Shen Y, *et al*. Immunosuppressive diterpenes from *Phomopsis* sp. S12 [J]. *Eur J Org Chem*, 2014, **2014**: 5728-5734.

[11] Hussain H, Krohn K, Ahmed I, *et al*. Phomopsinones A−D: four new pyrenocines from endophytic fungus *Phomopsis* sp. [J]. *Eur J Org Chem*, 2012, **2012**: 1783-1789.

[12] Hu ZX, Wu Y, Xie SS, *et al*. Phomopsterones A and B, two functionalized ergostane-type steroids from the endophytic fungus *Phomopsis* sp.TJ507A [J]. *Org Lett*, 2017, **19**: 258-261.

[13] Xu K, Zhang X, Chen JW, *et al*. Anti-inflammatory diterpenoids from an endophytic fungus *Phomopsis* sp.S12 [J]. *Tetrahedron Lett*, 2019, **60**: 151045.

[14] Chen HP, Huang MX, Li XW, *et al*. Phochrodines A−D, first naturally occurring new chromenopyridines from mangrove entophytic fungus *Phompsis* sp. 33 [J]. *Fitoterapia*, 2018, **124**: 103-107.

[15] Shang Z, Raju R, Salim AA, *et al*. Cytochalasins from an Australian marine sediment-derived *Phomopsis* sp. (CMB-M0042F): acid-mediated intramolecular cycloadditions enhance chemical diversity [J]. *J Org Chem*, 2017, **82**: 9704-9709.

[16] Huang MX, Li J, Liu L, *et al*. Phomopsichin A−D; four new chromone derivatives from mangrove endophytic fungus *Phomopsis* sp. 33 [J]. *Mar Drugs*, 2016, **14**: 215.

[17] Talontsi FM, Islam MT, Facey P, *et al*. Depsidones and other constituents from *Phomopsis* sp. CAFT69 and its host plant *Endodesmia calophylloides* with potent inhibitory effect on motility of zoospores of grapevine pathogen *Plasmopara viticola* [J]. *Phytochem Lett*, 2012, **5**: 657-664.

[18] Yan BC, Wang WG, Hu DB, *et al*. Phomopchalasins A and B, two cytochalasans with polycyclic-fused skeletons from the endophytic fungus *Phomopsis* sp. shj2 [J]. *Org Lett*, 2016, **18**: 1108-1111.

[19] Liu HX, Zhang L, Chen YC, *et al*. Cytotoxic pimarane-type diterpenes from the marine sediment-derived fungus *Eutypella* sp. FS46 [J]. *Nat Prod Res*, 2017, **31**: 404-410.

[20] Xu JL, Tan HB, Chen YC, *et al*. Lithocarpins A−D, four tenellone-macrolide conjugated [4 + 2] hetero-adducts from the deep-sea derived fungus *Phomopsis lithocapus* FS508 [J]. *Org Chem Front*, 2018, **5**: 1792-1797.

[21] Xu JL, Liu ZM, Chen YC, *et al*. Lithocarols A−F, six tenellone derivatives from the deep-sea derived fungus *Phomopsis lithocarpus* FS508 [J]. *Bioorg Chem*, 2019, **87**: 728-735.

[22] Chen SC, Liu ZM, Tan HB, *et al*. Tersone A−G, new pyridone alkaloids from the deep-sea fungus *Phomopsis tersa* [J]. *Mar Drugs*, 2019, **17**: 394.

[23] Xu JL, Liu HX, Chen YC, *et al*. Highly substituted benzophenone aldehydes and eremophilane derivatives from the deep-sea derived fungus *Phomopsis lithocarpus* FS508 [J]. *Mar Drugs*, 2018, **16**: 329.

[24] Cui H, Liu YN, Li J, *et al*. Diaporindenes A−D: four unusual 2, 3-dihydro-1*H*-indene analogues with anti-inflammatory activities from the mangrove endophytic fungus *Diaprothe* sp. SYSU-HQ3 [J]. *J Org Chem*, 2018, **83**: 11804-11813.

[25] Skehan P, Storeng R, Scudiero D, *et al*. New colorimetric cytotoxicity assay for anticancer-drug screening [J]. *J Nat Cancer Inst*, 1990, **82**: 1107-1112.

Cite this article as: LIU Hui-Bo, LIU Zhao-Ming, CHEN Yu-Chan, Tan Hai-Bo, LI Sai-Ni, LI Dong-Li, LIU Hong-Xin, ZHANG Wei-Min. Cytotoxic diaporindene and tenellone derivatives from the fungus *Phomopsis lithocarpus* [J]. *Chin J Nat Med*, 2021, **19**(11): 874-880.